J Mater Sci (2006) 41:5113–5121
DOI 10.1007/s10853-006-0071-2

Influence of scaffold meso-scale features on bone tissue response

Dianne Rekow · P. Van Thompson · John L. Ricci

Received: 29 November 2005 / Accepted: 24 March 2006 / Published online: 18 July 2006

Abstract Creation of bone to restore form and function following disease, growth disorders, and trauma is possible with bone-replacement scaffolds by controlling the complex sequence of new bone formation at the scaffold interface with the surrounding biologic milieu. Much is known about the influence of scaffold nano-scale (<1 μm) features on biocompatibility and the influence of micro-scale (1–20 μm) features on the type of tissue that develops. Meso-scale (20–1000 μm) features have been less well characterized, in part because it was not possible to regulate this feature size until solid freeform fabrication techniques became available. Experimental results of animal studies of bone ingrowth into scaffolds fabricated using these technologies confirm that meso-scale features can have profound effects on the extent and pattern of bone formation. They also indicate that we do not yet have sufficient information to optimize the size of these features. Macro-scale features (>1 mm) provide anatomic form and delimit the extent of the scaffold, serving as a platform to integrate other length-scale features. Many of the main effects of features at each length scale are understood but interactions across length scales still need investigation. Major improvements in bone replacement are now possible—but optimization of the process remains an as-yet unrealized goal.

Based on presentation: International Workshop on Interfaces: Interfaces by Design June 26–30, 2005.

D. Rekow (✉)
Department of Basic Science and Craniofacial Biology, NYU College of Dentistry, Room 1003 S, 345 East 24th Street, New York, NY 10010, USA
e-mail: edr1@nyu.edu

P. Van Thompson · J. L. Ricci
Department of Biomaterials and Biomimetics, NYU College of Dentistry, New York, NY, USA

Introduction

Disease, growth disorders, and trauma can be disfiguring and severely impact an affected person's quality of life. Restoration of form and function to the involved area often requires creating new tissue, including bone. Historically, this could only be accomplished by moving bone from one location of the skeleton into the defect site (autograft) or implanting treated bone from another human (allograft) or an animal (xenograft). All have associated limitations and risks. Now, using tissue engineering approaches and solid freeform fabrication technologies, scaffolds to support bone replacement can be created from an array of materials. With this, the challenge is to create designs to optimize tissue response.

Bone as a tissue is far more than just a simple set of like cells. Instead it is a dynamic and complex organization of active cells (including osteoblasts making new bone, mature osteoblasts, osteoclasts which remodel the bone in response to functional loading, and osteogenic cells which are undifferentiated and can become osteoblasts or osteoclats depending on the microbiologic conditions) and blood vessels to oxygenate the cells and clear away cellular debris and waste products. The multi-factorial, time-dependent sequence of formation of new bone incorporates recruitment and proliferation of cells with the potential of becoming bone

from stem cells circulating throughout the body and brought to a wound site in a blood clot, differentiation of those cells to become committed to forming bone, and then a progression of early bone (called osteoid), and a cascade of biochemical events resulting in mineralization, ultimately creating the composite structure we envision when we say bone [1]. This sequence is controlled by the interface and interactions between a scaffold and the surrounding biologic milieu [2].

In order to foster the growth of new bone, scaffolds must provide a template for cell interactions and structural support to newly forming tissue. As such, they must provide the required mechanical stability to support tissue development while having appropriate surface chemistry to be biocompatible; incorporate surface features to promote cell attachment, differentiation, and proliferation; have porosity to favor development of mature tissue with its supporting vasculature; and provide the proper external dimensions to fill a void and restore anatomic form. These functions are delivered by features across length scales ranging from sub-micron nano-scale to the millimeter macro-scale. Macro-scale features define the shape that is apparent when a scaffold is implanted. When the scaffold is needed in the head or face, the esthetic aspects it provides can significantly influence the patient's self image which has manifestations in their quality of life [3]. While these features may be the most important from a patient's perspective, they are not discussed in further detail here.

Nano-scale features of an implanted material with dimensions of less than 1 μm predominately control interactions at the protein level and are primarily responsible for biocompatibility. Materials interact with the body through highly specific recognition and binding sites between the cell and the scaffold material [4]. Immediately upon placement in the body, the material is coated with proteins, lipids, sugars, and ions from the extracellular fluid [5] that are essential for subsequent cell attachment and tissue development [6]. This cascade suggests that ''no material is truly inert'' [5]. Exceedingly small changes in the material can cause strikingly different reactions. A single carbon difference in the pendent chain of tyrosine-derived polycarbonates resulted in bone apposition falling from a frequency of 80% in the material to 17% in the altered material for 26 pins implanted for 270–1090 days in rabbits [7].

Requirements for biocompatibility testing are defined in a series of standards, the Tripartite Guidance, which includes International Organization for Standardization (ISO) 10933 standards (www.iso.org), the Biological Evaluation and Medical Devices standard developed by the American Association for the Advancement of Medical Instrumentation (AAMI at www.AAMI.org), and the U.S. Food and Drug Association (FDA) standard G95-1 (www.fda.org). Biocompatible bone-replacement scaffolds have been fabricated from ceramics, metals, polymers, and composites of materials. Much has been studied about interactions at this length scale and they are critically important but full discussion is beyond the scope of this review.

Micro-scale scaffold features, with dimensions in the range of 1–20 μm, modulate cell behavior, affecting both the type of cells that adhere to a scaffold surface and the directionality of cellular alignment. Smooth surfaces on early dental and orthopedic implants (metal, ceramic, *or* polymer) become encapsulated by fibrous tissue whereas rough surfaces promoted intimate bone contact (osseointegration) with the substrate material [8, 9]. Rough surfaces enhance platelet attachment [10] and fibrin clot adhesion [11], improving the stability of the scaffold-tissue interfaces during initial stages in the evolution of bone formation. Cells must attach to spread [12–15] and cell proliferation is stimulated by spreading [12–16]. Roughness, however, inhibits spreading. Instead, it drives the attached cells to a more enhanced state of differentiation. Proliferation and differentiation are inversely related. The challenge in scaffold design is to find the balance between these two competing phenomena, providing sufficient roughness for cell attachment while simultaneously promoting the spread of cells to create tissues throughout the entire volume of the scaffold while retaining or expressing the cell phenotype to create the required tissue type.

Interesting, the degree of roughness is critically important [5]. When osteoblasts are cultured on a smooth surface (with average surface roughness (R_a) < 0.2 μm), they assume a flat morphology like fibroblasts. If they are cultured on surfaces with R_a < 0.2 μm but peak-to-peak (R_m) greater than the length of the cell (approximately 10 μm), the surface is still perceived to be smooth and the cell assumes the same flat morphology. However, for surface features of R_a < 0.2 μm and R_m < 10 μm, the cells are unable to flatten and spread so instead they anchor to the extensions of multiple peaks and maintain their osteoblast morphology.

Features on the scaffold surface can control cell direction. This phenomenon, called contact guidance, was first described by Weiss in 1945 [17]. Orthogonal grooves in two areas of a substrate guide bone to develop bone with orientations that mimic the underlying geometry [18–20]. This is important because it

permits scaffold designs to tailor the orientation of developing tissues with the directionality ultimately needed for bearing loading stresses. One of the first practical applications of this was the use of dental endosseous (tooth replacement) implants with machined surfaces [20]. With modern technologies using lasers and photoetch processing, prescribed features can be created on the surface. The question, then, becomes, how can feature size be used to control tissue response?

Not surprisingly, as with roughness, feature size can dramatically affect tissue response. Features with dimensions of 1–15 μm, similar to the dimensions of the cell itself, are the most effective in eliciting the contact guidance response and ordered, periodic features are superior to random features in promoting bone attachment [18–20]. Laser micro-grooved titanium surfaces with 8–12 μm wide grooves limited cell spreading [21]. This technique has been shown to be effective in limiting soft tissue and bone attachment to specified areas in dental endosseous implants (see Fig. 1). Subtle differences are apparent in this example; epithelium (soft tissue) will not migrate across 8 μm grooves while 12 μm grooves fill with bone. Clinical studies confirm the effectiveness of the approach showing more intimate bone contact with the micro-grooved implant than with an adjacent implant of the same material and design but without the micro-gooves in the same patient [22].

Structural support and space to permit new tissue to develop is generally accomplished with features of meso-scale length of 200–1000 μm. For a number of reasons described below, this length scale has been largely overlooked. Yet features with this length scale (diameter and length of struts provide the structural support and shape, size, and interconnectivity of pores) are important for (1) controlling blood flow [23] as well as nutrient diffusion and flow of interstitial fluid [24] needed to control cell growth and function [25–27]; (2) manipulating tissue differentiation [28–31] and (3) optimizing both scaffold mechanical function [32] and mechanical properties of the regenerated tissue [33].

Solid free-form fabrication technologies have evolved, now providing possibilities of producing structures never before possible [34]. Using them, scaffold pore dimensions and interconnectivity (meso-scale features) to be controlled while simultaneously creating macro-scale anatomic form based on directly acquired 3D CT or MRI scan data [35, 36]. Together, the external form is complemented by an internal structure of meso- and micro-scale features [27, 37–39]. At least one practical application of this combined approach was demonstrated with a bone to replace a missing section of the lower arm [40].

The computer controlled solid freeform fabrication technologies bring new levels of control for meso-scale features. But also permits new questions to be addressed. For instance, what is the optimum pore size for bone ingrowth? Historically scaffolds could only be created from naturally occurring materials (e.g., specially treated coral) or by sponge-forming manufacturing methods (e.g., sol–gel, solution casting, high-pressure gas foaming with particulate leaching,

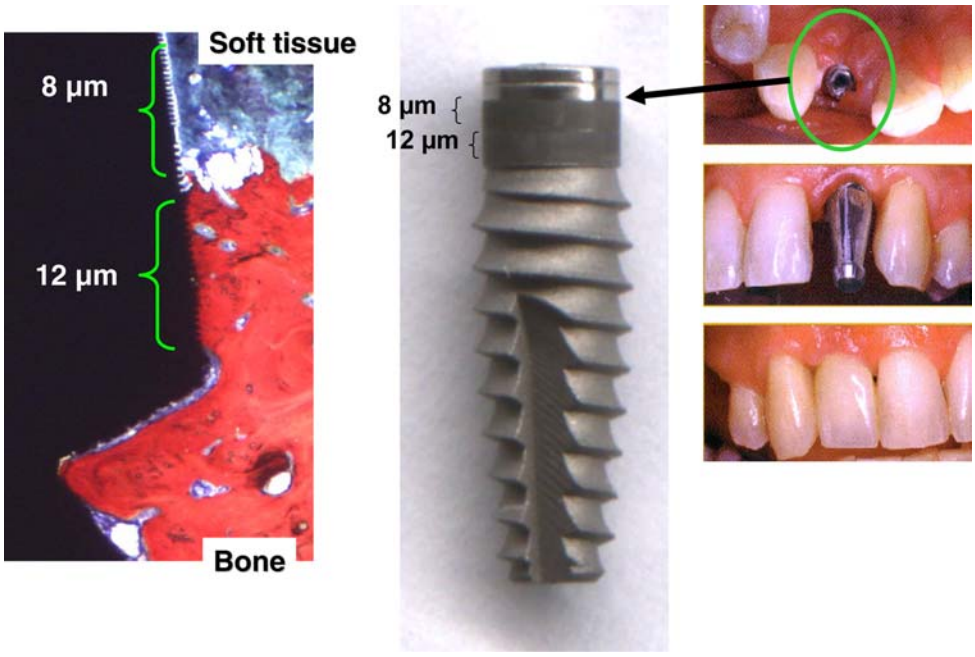

Fig. 1 Contact guidance using laser micro-grooves of different depth to control location and type of tissue attachment to a dental endosseous implant

etc.; see [41] for a comprehensive review). These all have random organization with multiple pore sizes and uncontrolled pore connectivity. This had made it difficult to quantify bone response to meso-scale features. Solid freeform fabrication technologies provided a platform to fabricate implants to explore bone response to features of this length scale. The objective of the experimental results reported here was to elucidate bone response to a series of scaffolds fabricated using solid freeform fabrication in various material-structure combinations.

Experimental method and materials

A series of scaffolds were created using solid freeform technologies with different material-structure combinations (shown in Figs. 2 and 3). Scaffolds 8 mm in diameter by 3 mm thick were fabricated by 3D printing [42, 43] and others 11 mm in diameter by 3 mm thick were fabricated using direct write assembly [44–46]. Three different designs were created in an attempt to determine the relationship between pore geometry and tissue response. One design (Fig. 2) was ''solid'' with four 750×750 μm pores extending form one flat surface to a depth of 2 mm plus four radial pores 750×750 μm pores at the outer circumference and extending through the sides of the scaffold. These were fabricated from polylactide-co-polyglycolide acid (PLGA, Birmingham Polymers, Inc., Birmingham, AL) and a tyrosine-based polycarbonate (poly-DTE, Integra LifeSciences, San Diego, CA) using 3D printing. A second design (Fig. 2), a ''waffle design'', consisted of orthogonal struts with 750 μm square cross section, creating a series of interconnected 500 μm pores. These were fabricated from poly-DTE using 3D printing. A third design (Fig. 3), also a ''waffle'', was created using direct-write assembly, permitting finer control of features size. Their design was similar to the waffle design created by 3D printing, but the flexibility of the technology permitted different combinations of pore sizes to be created in each quadrant of the scaffold. Struts of 250 μm and 400 μm were used to create two sets of scaffolds with this design with pore densities of 51–61% by volume. For each strut size, pore sizes of 250×250, 250×500, 500×500, 500×750, and 750×750 μm were created. The scaffolds shown in Fig. 3 were fabricated from hydroxyapatite ($Ca_{10}(PO_4)_6OH_2$; Reidel-de Haën, Germany) heat-treated at 400 °C for 1 h, 900 °C for 2 h and, finally, 1200 °C for 2 h, creating struts with 70% of their theoretical density.

Bone response to the scaffolds was tested in skulls of skeletally mature New Zealand White rabbits. Two 8-mm diameters holes were drilled in the parietal bones

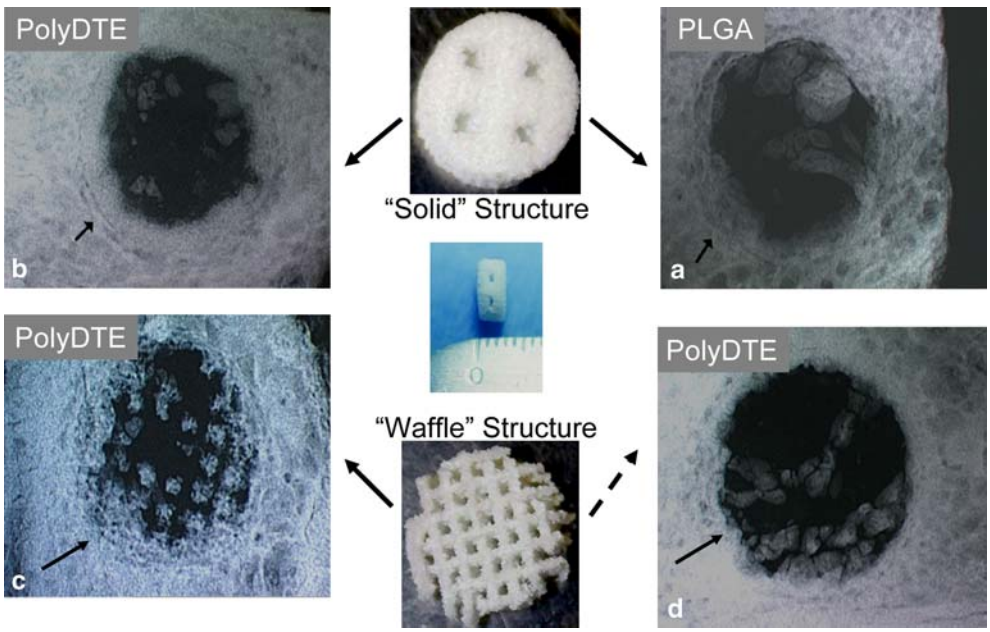

Fig. 2 Bone response to 3D printed scaffolds. ''Solid'' structures have pores from bottom (cranial) surface toward the top and radial pores through the entire diameter from the sides. ''Waffle'' structures have orthogonal struts forming an open network of interconnected porosity. (**a**) PLGA in ''solid'' scaffold with radial and bottom surface pores. (**b**) Same design as shown in (**a**) but fabricated from poly DTE. (**c**) Same material as shown in (**b**) but waffle design. (**d**) Same material and design as shown in (**c**) but struts collapsed before bone was mature enough to support itself. 10× magnification high resolution radiographs. Scaffold size is 8 mm diameter by 3 mm thick

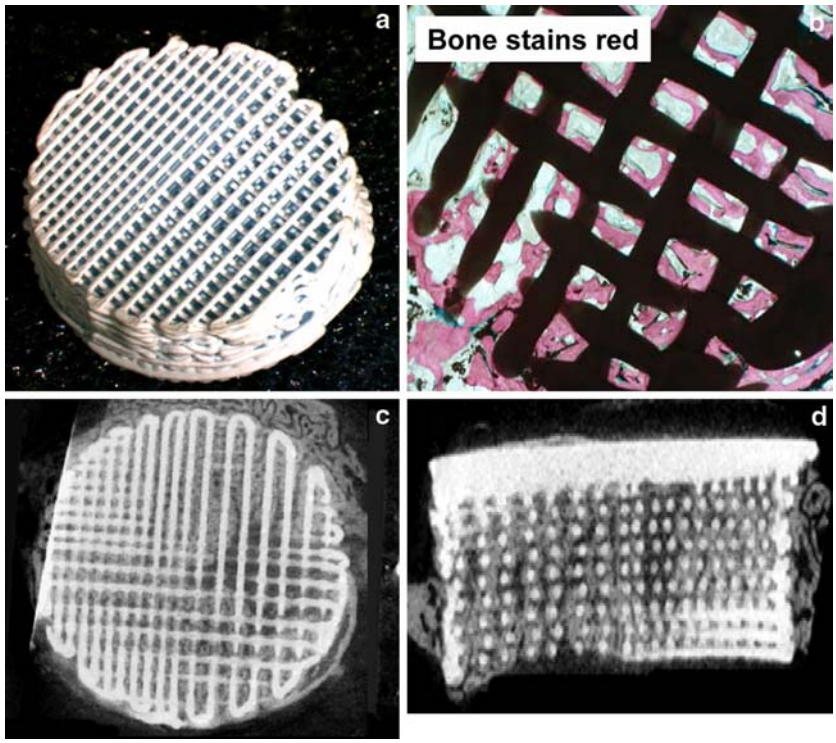

Fig. 3 Bone response to direct-write produced HA ''waffle'' scaffolds. (**a**) Pre-implanted scaffold with different strut-pore combinations within a single unit. Scaffolds are 11 mm diameter by 3 mm thick. (**b**) Histological section showing bone growth along the struts in a ''waffle'' structure. Bone stains red; scaffold struts are black (optical micro-graph of 8-week section). (**c** and **d**) Micro-CT images of scaffolds implanted for 8 weeks. Struts are white, bone is medium grey. Note that bone filled the majority of the scaffold space

on either side of the midline suture between the ears, creating trephine defects. This position was selected because it is among the most protected areas; the rabbit is unable to scratch it or irritate the area around the scaffold. The 8-mm diameter defects were smaller than critical size defects (defined as a defect that won't heal spontaneously [47, 48]). In previous studies with rabbits, when no scaffold was placed in this size defect, only a thin bridge of bone developed across the defect and this occurred in only a few cases. The new bone did not restore the original bone thickness. Thus, while some spontaneous fill was expected in the sub-critical size defects, the size permitted two scaffolds to be implanted in each animal (one on each side of the midline suture). After the defect was created, the scaffold was inserted; the periostium closed and sutured in place; and then the soft tissue was closed and sutured in place. At 6 weeks and 12 weeks, the rabbits were sacrificed and the implants and surrounding bone removed for radiographic and histomorphometric analysis (more complete details can be found in [42, 49, 50]).

Results and discussion

Bone response to 3D printed PLGA and poly-DTE scaffolds is shown in Fig. 2. In these a high resolution radiographic (faxitron) images, bone is light gray and the scaffold materials (and empty space) appear opaque. As expected, in all cases, bone grew from the periphery of the scaffold toward the center. However, there is a striking difference in the bone response within the scaffold between Fig. 2b and c. Both scaffolds were fabricated from the same material (poly-DTE), but the scaffold in Fig. 2c was the ''waffle'' design whereas the one in Fig. 2b was the ''solid'' design. With the ''waffle'' design, new bone developed from a number of locations *within* the scaffold, not just at the periphery. Clearly, the meso-scale scaffold features influenced the bone response. This finding suggests that by proper scaffold design, a defect could be filled with bone more quickly. This has the potential for important implications for clinical treatment.

While less dramatic, bone ingrowth was also shown to be influenced by the scaffold meso-scale features for the other, ''solid'' scaffold design. This design, fabricated from PLGA in Fig. 2a and polyDTE in Fig. 2b, directed bone ingrowth into the radial pores as well as in the square pores from the bottom surface. An important observation is that the material type did not appreciably influence the pattern of bone response.

The influence of meso-scale scaffold features is further evidenced by comparing bone response shown in Fig. 2c and d. Both scaffolds are the ''waffle'' design but the struts in the scaffold in Fig. 2d were created with lower density. During the healing time, many of the struts collapsed, destroying the meso-scale features. The resulting differences in bone response are

remarkable. Where the struts maintained their integrity (Fig. 2c and some located in the lower right corner of Fig. 2d), bone developed from the periphery as well as from a number of locations within the body of the scaffold. Where the struts collapsed (upper portion of the scaffold in Fig. 2d), the effect of the meso-scale features was lost.

Clearly meso-scale features influence bone response. The question that then arises is: what is the optimum meso-scale feature size for scaffolds? In particular, what pore size best serves the dual purpose of creating space for new bone (and life-supporting blood vessels) as well as clearance of cellular debris and/or breakdown products of biodegradable scaffolds? Does strut diameter or available surface area influence the extent of bone ingrowth?

Controversy about optimal pore size remains. Pore sizes of >300 μm are recommended for enhancing new bone formation [2] whereas mathematical models have suggested that 75 μm may be sufficient [51]. Studies in our laboratory with HA scaffolds suggests that blood vessels may develop in even smaller pores, at least in the short term [43]. Scaffolds were formed with parallel rods of HA using 3D printing. Depending on how the rods were laid down, pore sizes ranged from 15 μm to 40 μm. By 8 weeks, histological analysis showed evidence of developing blood vessels. This may suggest that prescribed, uniform meso-scale features like those that can be created with solid free-form fabrication may influence tissue response.

Our direct-write ''waffle'' scaffolds (Fig. 3) incorporated three different pore sizes within a single structure, permitting comparison of bone response to these meso-scale features in a single animal. Bone grew along and around the struts, filling available pores (Fig. 3b–d). It grew into the micro-scale pores (<10 μm) of the strut surface (indicated by the dark gray within the scaffold material at the interface between the two materials). Higher magnification images (Fig. 4) show that osteoblasts have aligned themselves along the struts (Fig. 4). Bone forms along the struts creating a continuous surface ''coating'' (Fig. 4b) and bone penetrates into the micro-porosity of the struts. The strength of the attachment is substantial. The specimen shown in Fig. 4b was imbedded in monomer and polymerization shrinkage occurs during processing. Rather than pulling the bone from the strut, the ceramic of the strut itself fractured (Fig. 4b) because of the shrinkage stresses, indicating the extensive bonding achieved between the bone and the ceramic.

Canaliculi emanating from the osteoblasts seen in Fig. 4a suggest that the dark areas along the strut are filled with cells and are not simply voids. This was confirmed at higher magnification backscatter images and by using X-ray micro-analysis calcium maps (Fig. 5). Bone ingrowth into the strut is shown in the backscatter image as dark gray in Fig. 5a and c. Extensive ingrowth is seen in Fig. 5c, indicated by the dark gray material within the strut. The associated X-ray micro-analysis maps calcium in both the HA of

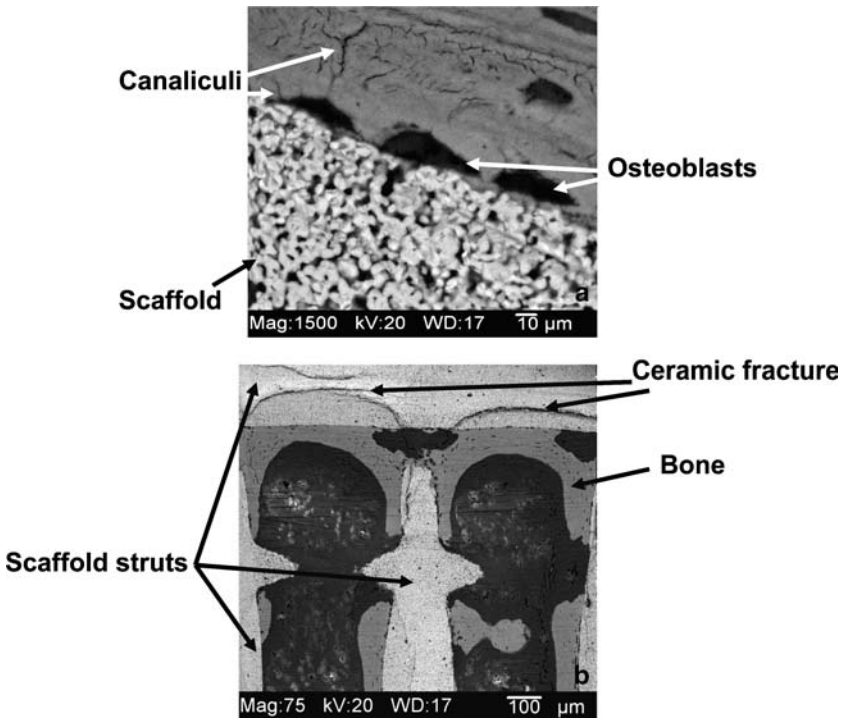

Fig. 4 Cross-sectional images of direct-write produced HA ''waffle'' scaffolds (SEM in backscatter mode). (**a**) Localized interfacial region showing bone cells (osteoclasts) along the strut with canaliculi extending from the cells and cellular processes penetrating into the micro-porosity of the strut. (**b**) Bone attaches around struts, changing direction when struts intersect. The strength of the attachment is sufficient to fracture the strut ceramic rather than the bone-strut interface when the embedding polymer shrank during processing

the strut itself and any bone that has grown into the micro-scale pores of the strut. The moth-eaten appearance of Fig. 5b reflects areas where no bone has grown into the micro-scale pores whereas the more continuous calcium distribution in Fig. 5d indicates that bone has filled many of the micro-scale pores. If the maps had reflected only calcium infiltration from body fluids, there would be no difference between these two calcium maps.

New bone developed throughout the entire volume of these HA ''waffle'' scaffolds. The amount of bone ingrowth was not substantially different for any of the pore-strut size combinations at 8 weeks or 16 weeks. While this is exceptionally good news, it fails to provide much insight into optimum size for meso-scale features and further studies are needed to elucidate the role of the pore and strut sizes. But there is a challenge in determining what the optimum meso-scale feature size should be. It is impossible to keep variables independent across length scales. Meso-scale scaffold features have an intrinsic surface texture (micro-scale feature) resulting from the fabrication technique and/or materials used. As an example, the scaffolds prepared from PLGA using 3D printing (Fig. 2) have a surface roughness substantially greater than that on the struts of the HA created by direct-write assembly and then ''smoothed'' by sintering (Fig. 3a). As described above, this micro-scale feature can influence tissue response. A major challenge in determining optimum feature size is to quantify the magnitude of main and interaction effects between meso- and micro-scale features.

Other challenges also exist. Bone is a dynamic and complex tissue. Its response to a scaffold can be modified by features at different length scales as described above. Bone matures and remodels over time and there is high potential for variation of the response between animals. Furthermore, limitations in existing evaluation tools make time-dependent local response of bone to scaffolds difficult to measure. Biochemical markers like transcription factors, bone morphogenic proteins, alkaline phosphatase, and osteopontin can provide insight into bone dynamics [52] but they are not site specific in living animals. Radiographic information is valuable but has limitations. Two-dimensional radiographs can mask important changes in different locations; 3D radiographs are expensive and difficult to obtain with high resolution

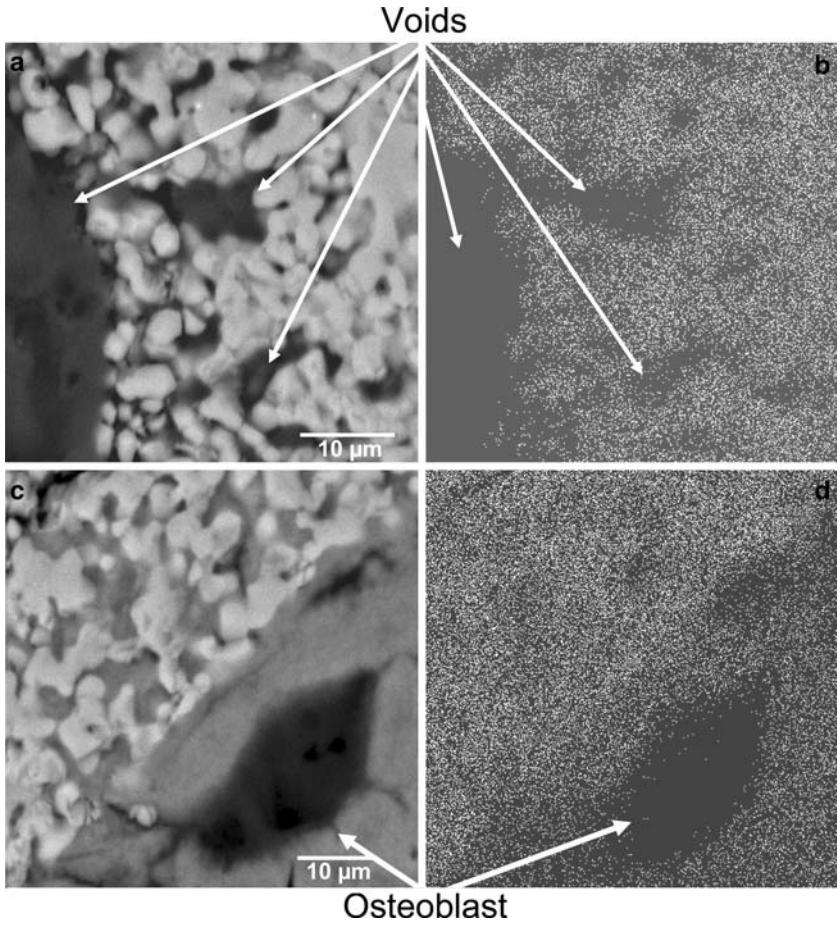

Fig. 5 Backscatter electron microscopy (**a** and **c**) and X-ray micro-analysis calcium maps (**b** and **d**) of edges of struts. Lightest gray in **a** and **c** is HA strut, medium gray is bone which has grown into the micro-scale pores of the strut. The calcium maps (**b** and **d**) show distribution of calcium in the sections, reflecting calcium in both the HA of the strut and any bone that has grown into the strut. Considerable bone in the pores of the struts, as see in **c**, creates calcium maps (**d**) which are different than the moth-eaten pattern of calcium (**b**) which reflects pores without bone ingrowth

on living animals. Histological analysis, the ''gold standard'' for tissue response requires that the animal be sacrificed.

Experiments confirm that bone response to scaffolds can be modified by scaffold features and the patterns of response influenced by meso-scale features. To truly tailor the tissue response—and to move to controlling hard and soft tissue response—we need further understanding of the interactions within and across length scales.

Summary

Scaffold features at different length scales can have dramatic influence on bone tissue response. Nano-scale features influence biocompatibility. Micro-scale features affect the types and orientation of tissues that develop within the scaffold. Meso-scale features influence the structural support of the scaffold and the amount of bone that can develop. Largely overlooked until now, they can have substantial influence on the pattern of bone that develops. That, in turn, can influence the fill rate of the scaffold with important clinical implications. Macro-scale features establish the anatomic form and can dramatically influence a patient's self image. Main effects of each length scale have been addressed but interactions between features across length scales are still needed to optimize bone response. Major improvements in bone replacement are now possible—but optimization of the process remains an as-yet unrealized goal.

Acknowledgements The research reported here could only have been accomplished through support by graduate students Tithi Dutta Roy and Josh Simon and collaboration of Dr. Kathleen Chesmel at Therics for 3D printing, and Drs. Jennifer Lewis at University of Illinois at Chicago and James Smay at the Oklahoma State University for direct-write assembly of scaffolds.

References

1. Aubin J (2001) Rev Endocr Metab Disord 2:81
2. Karageorgiou V, Kaplan D (2005) Biomaterials 26:5474
3. Girotto JA, Mackenzie E, Fowler C, Redett R, Robertson B, Manson PN (2001) Plast Reconstr Surg 108:312
4. Ratner B (1993) J Biomed Mater Res 27:837
5. Boyan B, Schwartz Z (2000) In: Bone Engineering. em squared incorporated, Toronto, p 232
6. Adams J (2002) Exp Rev Mol Med 11. Preprint at http://www.ermm.cbcu.cam.ac.uk/02004039h.htm as on September 16, 2005
7. James K, Levene H, Kaufmann E, Parsons J, Kohn J (2000) In: Bone Engineering. em squared incorporated, Toronto, p 195
8. Albrektsson T, Hansson HA, Ivarsson B (1985) Biomaterials 6:97
9. Thomas KA, Cook SD (1985) J Biomed Mater Res 19:875
10. Davies JE (1998) Int J Prosthodont 11:391
11. Gemmell C, Park J (2000) In: Bone Engineering. em squared incorporated, Toronto, p 108
12. Chen CS, Mrksich M, Huang S, Whitesides GM, Ingber DE (1997) Science 276:1425
13. Dike LE, Chen CS, Mrksich M, Tien J, Whitesides GM, Ingber DE (1999) In Vitro Cell Dev Biol Anim 35:441
14. Ingber D, Madri J, Al E (1986) Endocrinology. 119:1768
15. Re F, Zanetti A, Al E (1994) J Cell Biol 127:537
16. Folkman J, Moscona A (1978) Nature 273:345
17. Weiss L (1945) J Exp Zool 100:353
18. Brunette DM, Chehroudi B (1999) J Biomech Eng 121:49
19. Clark P, Connolly P, Curtis AS, Dow JA, Wilkinson CD (1991) J Cell Sci 99:73
20. Ricci JL, Charvet J, Frenkel SR, Chang R, Nadkarni P, Turner J, Alexander H (2000) In: Bone Engineering. em squared incorporated, Toronto, p 282
21. Soboyejo W, Nemetski B, Allameh S, Nmarcantonio N, Mercer C, Ricci J (2002) J Biomed Mater Res 65:56
22. Alexander H, Pecora G, Guarnieri R, Ceccarelli R, Ricci JL (2004) Presented at Academy of Osseointegration Annual Meeting, San Francisco, March 18–20, 2004 (winner of the 2004 Clinical Innovations Award)
23. Kuboki Y, Takita H, Koboyashi D, Tsuruga E, Inoue M, Murata M, Nagai N, Dohi Y, Ohgushi H (1998) J Biomed Mater Res 39:190
24. Hui P, Leung PC, Sher A (1996) J Biomech 29:123
25. Cima L, Vacanti J, Vacanti C, Ingber D, Mooney D, Langer R (1991) J Biomech Eng ASME 113:143
26. Freyman T, Yannas I, Gibson L (2001) Prog Mater Sci 46:273
27. Zeltinger J, Sherwood J, Graham D, Mueller R, Griffith L (2001) Tissue Eng 7:557
28. Gauthier O, Bouler J, Aguardo E, Pilet P, Daculsi G (1998) Biomaterials 19:133
29. Holmes R, Bucholz R, Mooney V (1986) J Bone Jt Surg Am 68A:904
30. Shors E (1999) Orthop Clin North Am 30:599
31. Tsuruga E, Takita H, Itoh H, Wakisaka Y, Kuboki Y (1997) J Biochem 121:317
32. Le Huec J, Schaevereke T, Clement D, Faber J, Le Rebeller A (1995) Biomaterials 16:113
33. Martin R, Chapman M, Sharkey N, Zissimos S, Bay B, Shors E (1993) Biomaterials 14:341
34. Charriere E, Lemaitre J, Zysset P (2003) Biomaterials 24:809
35. Berry E, Brown JM, Connell M, Craven CM, Efford ND, Radjenovic A, Smith MA (1997) Med Eng Phys 19:90
36. Wilson CE, De Bruijn JD, Van Blitterswijk CA, Verbout AJ, Dhert WJ (2004) J Biomed Mater Res 68A:123
37. Chu TM, Orton DG, Hollister SJ, Feinberg SE, Halloran JW (2002) Biomaterials 23:1283
38. Hutmacher DW, Sittinger M, Risbud MV (2004) Trends Biotechnol 22:354
39. Zeltinger J, Sherwood JK, Graham DA, Mueller R, Griffith LG (2001) Tissue Eng 7:557
40. Mulligan T (2003) Plasti-Bone, http://www.onr.navy.mil/media/article. asp?ID-59 as on October 29, 2005
41. Agrawal CM, Ray RB (2001) J Biomed Mater Res 55:141
42. Roy TD, Simon JL, Ricci JL, Rekow ED, Thompson VP, Parsons JR (2003) J Biomed Mater Res 67A:1228
43. Roy TD, Simon JL, Rekow ED, Ricci JL, Thompson VP, Parsons JR (2004) J Biomed Mater Res 67A:1228
44. Smay JE, Cesarano J, Lewis J (2002) Langmuir 18:1639

45. Smay JE, Cesarano J III, Lin SY, Stueker JN, Lewis JA (2001) In: Solid freeform fabrication symposium proceedings, p 175
46. Lewis J, Gratson GM (2004) Materials Today (July/August, 2004)
47. Hollinger JO, Kleinschmidt JC (1990) J Craniofac Surg 1:60
48. Schmitz JP, Hollinger JO (1986) Clin Orthop Relat Res 205:299
49. Simon JL, Roy TD, Parsons JR, Rekow ED, Thompson VP, Kemnitzer J, Ricci JL (2003) J Biomed Mater Res 66A:275
50. Roy TD, Simon JL, Rekow ED, Ricci JL, Parsons JR (2004) J Biomed Mater Res 66A:283
51. Skinner HB (1979) Med Inform (Lond) 4:43
52. Sodek J, Cheifetz S (2000) In: Bone Engineering. em squared incorporated, Toronto, p 31